P2X receptor signaling inhibits BDNF-mediated spiral ganglion neuron development in the neonatal rat cochlea

Denise Greenwood[1], Daniel J. Jagger[2], Lin-Chien Huang[1], Noriyuki Hoya[1], Peter R. Thorne[3], Scott S. Wildman[4], Brian F. King[4], Kwang Pak[5], Allen F. Ryan[5,6] and Gary D. Housley[1,*]

Type I and type II spiral ganglion neurons (SGN) innervate the inner and outer hair cells of the cochlea, respectively. This neural system is established by reorganization of promiscuous innervation of the hair cells, immediately before hearing is established. The mechanism for this synaptic reorganization is unresolved but probably includes regulation of trophic support between the hair cells and the neurons. We provide evidence that P2X receptors (ATP-gated ion channels) contribute such a mechanism in the neonatal rat cochlea. Single-cell quantitative RT-PCR identified the differential expression of two P2X receptor subunits, splice variant P2X$_{2-3}$ and P2X$_3$, in a 1:2 transcript ratio. Downregulation of this P2X$_{2-3/3}$ receptor coincided with maturation of the SGN innervation of the hair cells. When the P2X$_{2-3}$ and P2X$_3$ subunits were co-expressed in *Xenopus* oocytes, the resultant P2X receptor properties corresponded to the SGN phenotype. This included enhanced sensitivity to ATP and extended agonist action. In P4 spiral ganglion explants, activation of the P2X receptor signaling pathway by ATPγS or α,βMeATP inhibited BDNF-induced neurite outgrowth and branching. These findings indicate that P2X receptor signaling provides a mechanism for inhibiting neurotrophin support of SGN neurites when synaptic reorganization is occurring in the cochlea.

KEY WORDS: Spiral ganglion neuron, ATP-gated ion channel, Neurotrophins, BDNF, Synaptic reorganization, Afferent development

INTRODUCTION

In rodent models, such as the rat, where detection of airborne sound commences at around postnatal day 11 (P11) (Geal-Dor et al., 1993), it has been established that the afferent innervation of the cochlea arises from a programmed pattern of neurite outgrowth to the sensory hair cells, followed by selective pruning in the week prior to the onset of hearing (Simmons et al., 1991). The molecular mechanism for rationalization of afferent neurite extension and branching that leads to the mature cochlear innervation pattern has not been established, but occurs in the face of ongoing trophic support from the hair cell-derived neurotrophins.

In the mature mammalian cochlea, 90-95% of the primary afferent fibers innervate individual inner hair cells (IHCs). The remaining 5-10% of the cochlear afferents have neurites that branch extensively to synapse with multiple outer hair cells (OHCs). These are the type I and type II spiral ganglion neurons (SGN), respectively (Berglund and Ryugo, 1987). The IHC-type I SGN pathway represents the principal channel for sound transduction and auditory neurotransmission, with each IHC supporting exclusive synapses with many type I SGN. The function of the OHC-type II SGN pathway has not been determined but is likely to provide sensory feedback from the cochlear amplifier, which is an active tuning process that supports the sensitivity and frequency selectivity of the hearing organ (e.g. Jagger and Housley, 2003). Thus, the more numerous type I SGN

initially innervate both IHC and OHC, and subsequent pruning of these connections results in withdrawal of redundant neurites from the OHC and refinement of the innervation at the IHC. Type II SGN initially innervate both IHC and OHC, with subsequent loss of the IHC connections (see Fig. 1) (for reviews, see Pujol et al., 1998; Rubel and Fritzsch, 2002). Neurotrophins, particularly brain-derived neurotrophic factor (BDNF) and NT3, are secreted by the hair cells and act as survival factors for SGN. They may also promote neurite extension and branching during synaptogenesis in the cochlea (Mou et al., 1997; Pirvola and Ylikoski, 2003). Expression of the neurotrophins BDNF and NT3 by the hair cells and their respective receptors, TRKB and TRKC, by the SGN is established as neurite outgrowth from the spiral ganglion commences (at around E18.5) and is sustained through the neurite pruning that establishes the mature cochlear afferent innervation pattern (Pirvola and Ylikoski, 2003).

Candidates for signal transduction pathways that contribute to regulation of axon growth and synaptic determination include traditional axon guidance molecules, and also several neurotransmitters such as glutamate, acetylcholine and adenosine 5′-triphosphate (ATP) (Huang et al., 2006). ATP mediates cell signaling through activation of two classes of purinergic receptor, the metabotropic P2Y receptor and the ionotropic P2X receptor. The P2X receptor family (P2X$_1$-P2X$_7$) has wide distribution among neural systems, including the inner ear (Khakh and North, 2006). ATP-gated ion channel diversity arises from heteromeric assembly and alternative splicing of the P2X receptor subunits. P2X$_3$ receptors have been shown to inhibit motor axon outgrowth in neural tube explants (Cheung et al., 2005). We have now established that P2X$_3$ receptor expression is prominent in rat and mouse SGN and has a spatiotemporal expression pattern that matches the early postnatal period of neurite reorganization (Huang et al., 2005; Huang et al., 2006). Trafficking of the P2X$_3$ receptor protein matched the timing of cochlear afferent synaptic restructuring prior to the onset of hearing. In the first few postnatal days in the rat, P2X$_3$ immunolabeling in the neurite terminals was confined to the

[1]Department of Physiology, University of Auckland, Private Bag 92019, Auckland, New Zealand. [2]Centre for Auditory Research, University College London, London, UK. [3]Audiology Discipline, University of Auckland, Private Bag 92019, Auckland, New Zealand. [4]Department of Physiology, University College Medical School, University College London, London, UK. Departments of [5]Surgery and [6]Neuroscience, University of California, San Diego, 9500 Gilman Drive, La Jolla, San Diego, CA 92093, USA.

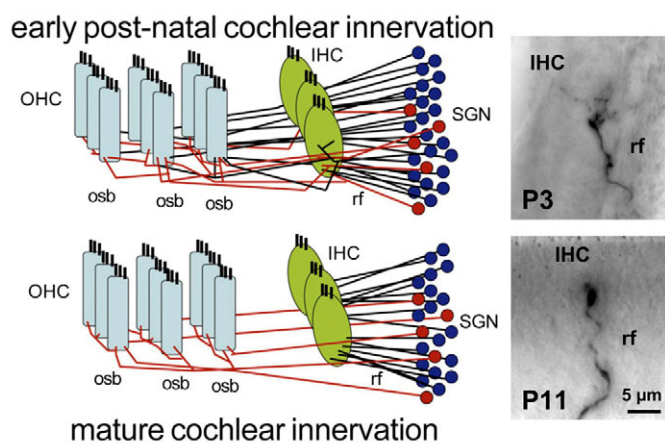*Author for correspondence (e-mail: g.housley@auckland.ac.nz)

Fig. 1. Immature and mature configurations of the afferent innervation of the cochlea by the intrinsic SGN. (Top) In the early postnatal (P3) rat cochlea, type I and type II SGN innervation is mismatched with target hair cells. (Bottom) By the onset of hearing (around P11), several type I SGN neurites (blue) exclusively innervate individual inner hair cells (IHC) with pruning of the synaptic processes to a few puncta. By contrast, the considerably less numerous type II SGN neurites (red) drop their innervation of the IHC and provide extensive en passant innervation of multiple outer hair cells (OHC) through the outer spiral bundles (osb). rf, radial fibers. Spiral ganglion neurite outgrowth is promoted by neurotrophins, particularly BDNF, which is a paracrine factor secreted by the hair cells. Here we provide evidence that extracellular ATP signaling acts through a P2X$_{2/3}$ heteromeric receptor to inhibit this neurotrophic support.

inner spiral plexus-IHC region, then extended to include tunnel-crossing afferents innervating the OHC. P2X$_3$ expression was then downregulated under the IHC by P8, and lost from the outer spiral bundle fibers innervating the OHC by P14 (Huang et al., 2005). This contrasts with the sustained P2X$_2$ receptor expression in both the inner radial fibers and the outer spiral fibers in the developing rat cochlea (Järlebark et al., 2000). The other five P2X receptor subunits in the rat SGN exhibit variable expression (Xiang et al., 1999; Nikolic et al., 2001; Nikolic et al., 2003), with P2X$_1$ downregulating from P2 (Nikolic et al., 2001). To date, no other candidate neurohumoral signal transduction pathways such as the glutamate receptors or neurotrophin receptors show the coincident expression profile of the P2X$_3$ receptor. P2X receptors containing the P2X$_3$ subunit therefore represent a candidate molecular signaling pathway, which may complement neurotrophic support and reshape the afferent innervation of the cochlear hair cells.

Spiral ganglion neurons of the neonatal rat cochlea express ATP-gated ion channels with a unique P2X receptor phenotype. Features of this P2X receptor include unusual sensitivity to ATP and broad agonist action, which shows some semblance of both P2X$_2$ and P2X$_3$ phenotype but cannot be readily reconciled with published data for recombinant P2X$_{2/3}$ receptor heteromers (Salih et al., 2002). P2X$_2$, P2X$_3$ and P2X$_{2/3}$ receptors contribute to transduction and neurotransmission in a range of sensory modalities (for reviews, see Khakh and North, 2006; North, 2002), with alternative splicing potentially broadening receptor diversity (Brändle et al., 1997; Salih et al., 1998).

The present study undertook a molecular characterization of the P2X receptors expressed by the rat neonatal SGN during the crucial period for neural reorganization immediately prior to the onset of hearing. Using quantitative single-cell RT-PCR, we found

that the P2X$_3$ subunit was the dominant transcript, with approximately 50% greater abundance than the P2X$_2$ subunit; compatible with a P2X$_3$-P2X$_3$-P2X$_2$ trimer assembly (Jiang et al., 2003). The other five P2X receptor transcripts were less abundant. Alternative splicing of the P2X$_2$ receptor was apparent, with dominance of a P2X$_{2-3}$ isoform (Salih et al., 1998). The pharmacological properties of the recombinant P2X$_{2-3/3}$ heteromer, expressed in *Xenopus* oocytes, matched the native SGN P2X receptor phenotype. This pharmacological profile was exploited in a neonatal spiral ganglion explant model to demonstrate that ATP, acting through this P2X receptor, counters the neurite extension and branching elicited by the neurotrophin BDNF. These findings establish a mechanism contributing to the pruning and withdrawal of neurites contacting the sensory hair cells, which is required for the reorganization of cochlear synaptic innervation as hearing is established.

MATERIALS AND METHODS

Gene transcript analysis
RT-PCR
Total RNA was extracted from spiral ganglia dissected from cochleae of Wistar rats at postnatal ages P0-P4 inclusive and P14, using Trizol (Invitrogen). Reverse transcription was performed on 0.5 µg total RNA using random hexamers and Superscript II (Invitrogen) in a 20 µl reaction mix. A non-quantitative PCR amplification for all the P2X receptors was performed on cDNA samples (4 µl) in a reaction volume of 50 µl containing 1× PCR buffer, 2 mM MgCl$_2$, 200 µM dNTPs, 200 nM each of forward and reverse primers and 1 U AmpliTaq Gold DNA polymerase (Perkin-Elmer). PCR amplification included denaturation at 96°C for 5 minutes, then 48 cycles of 94°C for 45 seconds, 58°C for 45 seconds and 72°C for 90 seconds, followed by 72°C for 10 minutes. Samples (10 µl) of PCR product were analysed by agarose gel electrophoresis. Each experiment consisted of the P2X receptor target in duplicate. Controls included omission of the reverse transcriptase reaction or no cDNA template. The procedure was repeated using cDNA derived from two independent rat spiral ganglia (a summary of PCR primers is given in Tables 1 and 2).

Single-cell PCR analysis
Cochlear slices were prepared from neonatal rats (P2-P4) as described by Jagger et al. (Jagger et al., 2000). SGN were aspirated into glass micropipettes (GC120TF-10; Clark Electromedical Instruments, UK) containing 2 µl of sterile 0.1 M PBS. In some instances cells were aspirated into recording pipettes following voltage-clamp analysis of P2X receptor currents (see 'patch clamp of SGN' section). The contents of the electrode were immediately expelled into a chilled, thin-walled silicon-coated 0.5 ml microfuge tube (Invitrogen) containing 9 µl of RT reaction mixture (1× RT buffer, 150 ng random hexamers, 1 mM dNTPs, 20 U RNAseOut; Invitrogen). Cells were stored at –80°C for 1 hour and then thawed on ice to promote lysis. Cells were incubated at 65°C for 10 minutes, then cooled to 25°C before the addition of 0.5 µl Superscript II reverse transcriptase. Reverse transcription proceeded for 10 minutes at 25°C, then 1 hour at 42°C, followed by inactivation at 70°C for 10 minutes. cDNAs not used immediately were stored at –80°C. Controls included RT-PCR of bath solution collected adjacent to SGN, no template controls and omission of reverse transcription for SGN mRNA samples.

Real-time PCR assay for single-cell transcript quantification
Real-time quantification of mRNAs for P2X receptor and the control genes glyceraldehyde-3-phosphate dehydrogenase (*Gapdh*) and neuron-specific enolase [(*Nse*), also known as *Eno2* – Mouse Genome Informatics] was performed using gene-specific primers and TaqMan fluorogenic MGB probes. The oligonucleotide primers and TaqMan MGB probes (Tables 1 and 2) were designed using Primer Express v1.5 (PE Applied Biosystems).

Table 1. Primer sequences for standard PCR reaction

Target	Sense (5'-3')	Antisense (5'-3')	bp	GenBank
P2X$_1$	TATGTGGGTGCGAGAGTCAGG	TCCTCATGTTCTCCTGCAGG	493	X80477
P2X$_2$	GCATGGACAGGCAGGGAAAT	GGGAAAGGAGATGGCAGGGAAC	689	U14414
P2X$_2$ (internal)	CGGGGTGGGCTCCTTCCTGT	GGACATGGTTACTGAAGAGCG	499	U14414
P2X$_3$	CACCATTATCAGCTCGGTGG	GTGTGGAAGTGCTTGGTACG	556	X91167
P2X$_4$	CTTCATCATGACCAACATGAT	GTGGTGATGTTGGGGAGGGA	343	X91200
P2X$_5$	GCTGGGGAGTCTGTGTTGTA	CTCGGTAAAACTCACTC	685	X92069
P2X$_6$	TCCTTCTTCCTGGTAACCAAC	TGTTGTCCCAGGTATCTAAGG	341	X92070
P2X$_7$	GAGGCTAACAACTTCCAATTCCTG	CAGATTACATGGCAAGCTCACCC	890	X95882
NSE	TGGCTACACGGAAAAGATGGTG	CCTTGAGCAGCAAACAGTTGC	308	M1193
GAPDH	CCTGCACCACCAACTGCTTAGC	GAGTTGCTGTTGAAGTCACAG	417	X02331

The real-time PCR reaction was performed using an ABI 7700 Sequence Detection System (PE Applied Biosystems). The reaction mixture (25 μl) consisted of a 2 μl sample of neuron cDNA (as a 1:1 dilution of the first-strand cDNA synthesis reaction, see above), 750 nM of each primer, 200 nM of TaqMan MGB probe and 1× TaqMan Universal PCR MasterMix (PE Applied Biosystems). PCR amplification was performed for 2 minutes at 50°C, heated to 95°C for 10 minutes and then followed by 50 cycles of 15 seconds at 95°C and 1 minute at 60°C. Standard curves for each gene target were generated by amplification using conventional PCR to produce larger amplicons flanking the real-time PCR targets. These PCR products were purified by Qiagen gel extraction (Qiagen) from 1.5% agarose gels. The DNA concentration (ng/μl) was determined by UV spectrometry and the starting copy number calculated, providing the basis for serial dilution down to single-copy equivalence. Standard curves were derived from plotting cycle threshold (C_T) against copy number (using the 10,000 to single-copy standard dilution series) in triplicate. Each experiment contained a series of negative and positive controls, including no template controls, bath solution, negative tissues and omission of reverse transcription. Transcript numbers were expressed as the mean±s.e.m. Statistical significance among different P2X receptor transcript numbers was assessed by one-way analysis of variance (ANOVA) and post-hoc Student's paired *t*-tests.

Validation of a single-cell real-time PCR assay

The single-cell real-time PCR method employed here was designed to allow quantification of nine different gene transcripts from individual SGN at low copy number. This approach required division of the cDNA derived from each neuron to provide a sufficient template for multiple PCRs. Using this approach, the relative abundance and not the absolute copy number of each transcript was sought, such that our methodology establishes the proportional representation of specific transcripts relative to each other, based on real-time PCR utilizing TaqMan chemistry (Bustin, 2002).

In control experiments we initially confirmed the specificity of the primer/probe sets by performing PCRs using specific P2X receptor subunit cDNA templates with all primer/probe combinations. The lack of amplification of off-target templates up to 50 cycles confirmed the specificity of the PCRs (Fig. 2A,B). Standard curves using dilutions of the cDNA templates confirmed reproducibility and sensitivity of the PCR protocol. A standard curve of copy number against C_T value was generated from these data and the linear regression equation $y=mx+c$ was derived for quantification of single-cell P2X receptor gene copies. This analysis showed

that the standard curves from the dilution series were linear to <10 copies (Fig. 2C). Analysis of each dilution series enabled determination of the detection limit, slope and PCR efficiency of each reaction (Fig. 2D) and therefore the reproducibility and reliability of using interpolation from the standard curves to quantify multiple gene transcripts amplified from the same neuron. For each target, the slope of the standard curve approximated –3.32, the theoretical value representing a PCR reaction where the number of template molecules double with each cycle and hence are 100% efficient (Ginzinger, 2002; Pfaffl et al., 2002).

End-point RT-PCR of P2X$_2$ splice variants

A first round of PCR amplification was performed in 50 μl using 5 μl of cDNA template, with 1× PCR buffer, 2 mM MgCl$_2$, 200 mM dNTPs, 10 nM primers and 1 U AmpliTaq Gold polymerase (PE Applied Biosystems) for 30 cycles of 30 seconds at 94°C, 45 seconds at 60°C and 90 seconds at 72°C, followed by 7 minutes at 72°C. A second round of PCR was performed using 4 μl of first-round product as a template (final volume 25 μl). In this second PCR, the P2X$_2$ splice variants were amplified using a second set of internal primers (100 nM each) and by performing 46 PCR cycles as described above. The internal PCR primers designed for P2X$_2$ (Accession No. U14414) semi-nested single-cell PCR are included in Table 1. Neurons were processed in batches of six, and positive and negative controls were included. Amplicons were verified by agarose gel electrophoresis.

Immunohistochemistry

Cochleae dissected from neonatal P4 rat pups were fixed in 4% formaldehyde and 0.5% gluteraldehyde in 0.1 M phosphate buffer (pH 7.4) for the P2X$_2$ antibody and 4% paraformaldehyde in 0.1 M phosphate buffer (pH 7.4) for the P2X$_3$ and P2X$_4$ antibodies. Tissues were cryoprotected and sectioned as previously described (Huang et al., 2005; Järlebark et al., 2000). After a series of washes in 0.1 M PBS, sections were incubated for 2 hours at room temperature in a blocking-permeabilization solution of 10% normal goat serum (Vector Laboratories) and 1% Triton X-100 in 0.1 M PBS. Primary antibody was applied in 10% normal goat serum and 0.1% Triton X-100 at dilutions of 1:500 for P2X$_2$, 1:30,000 for P2X$_3$ and 1:200 for P2X$_4$ and incubated overnight at 4°C. Primary antibody was removed by 0.1 M PBS washes. Sections were incubated with secondary antibody (Alexa Fluor-594) at 1:500 for 2 hours at room temperature and 2 hours at 4°C. Secondary antibody was removed by 0.1 M PBS washes as described but with an additional incubation in PBS overnight at 4°C. Sections were mounted in Citifluor (Agar Scientific, UK) on microscope slides (ProbeOn Plus; Fisher Scientific, Pittsburgh, PA). Immunofluoresence images were

Table 2. Primer and probe sequences for quantitative PCR reaction

Target	Sense (5'-3')	Antisense (5'-3')	Probe
P2X$_1$	GCTGATGGCTTGAGCCAG	TGGTGTCGCCTTGCAGGA	6FAM-AGAGGGCATTCCCA
P2X$_2$	TCGACAAGGTGCGTACTCCA	GGCAAGGGTCACAGGCC	6FAM-AGCATCCCTCAA
P2X$_3$	GCAGCGTACCGCACACT	ACCAGCACATCAAAGCGGA	6FAM-CTGAAGGCTTTGGC
P2X$_4$	TGCAACCTGGATAGAGCC	GGCGCCGGAAGGAATATCT	6FAM CTCCCTTTGCCTGCC
P2X$_5$	AGGCAGGGAAAATTCAGCATCA	CGCCAGCCCAGAACCA	6FAM-CCCACAGTCATCAAC
P2X$_6$	AACCAACTTCCTTGTGACACCA	GGAACAAGGATGCTCTGGG	6FAM-TCAAGTCCAGGGCAGAT
P2X$_7$	GAGACGAACTGCGCATGTCA	TCCCCACATGTAACGACAAGG	6FAM-AGAGGACCACTCTGCT
NSE	CCGCGATGGCAAATACG	TGCATCGGGTTGGGTCA	6FAM-CTTGGATTTCAAGTCTCC
GAPDH	TGACAACTTTGGCATCGTGG	CACAGTCTTCTGAGTGGCAGTGAT	6FAM-ATGACCACAGTCCATG

A

B

P2X Primers and Probes

	P2X1	P2X2	P2X3	P2X4	P2X5	P2X6	P2X7
P2X1	24.86	—	—	—	—	—	—
P2X2	—	24.8	—	—	—	—	—
P2X3	—	—	24.96	—	—	—	—
P2X4	—	—	—	25.8	—	—	—
P2X5	—	—	—	—	25.57	—	—
P2X6	—	—	—	—	—	27.8	—
P2X7	—	—	—	—	—	—	26.22

Ct value: P2X targets @ 10^4 molecules/μl

C

P2X$_1$ Standard Curve

$y = -1.4032\mathrm{Ln}(x) + 36.78$
$R^2 = 0.9988$

D

Standard Curve Analysis

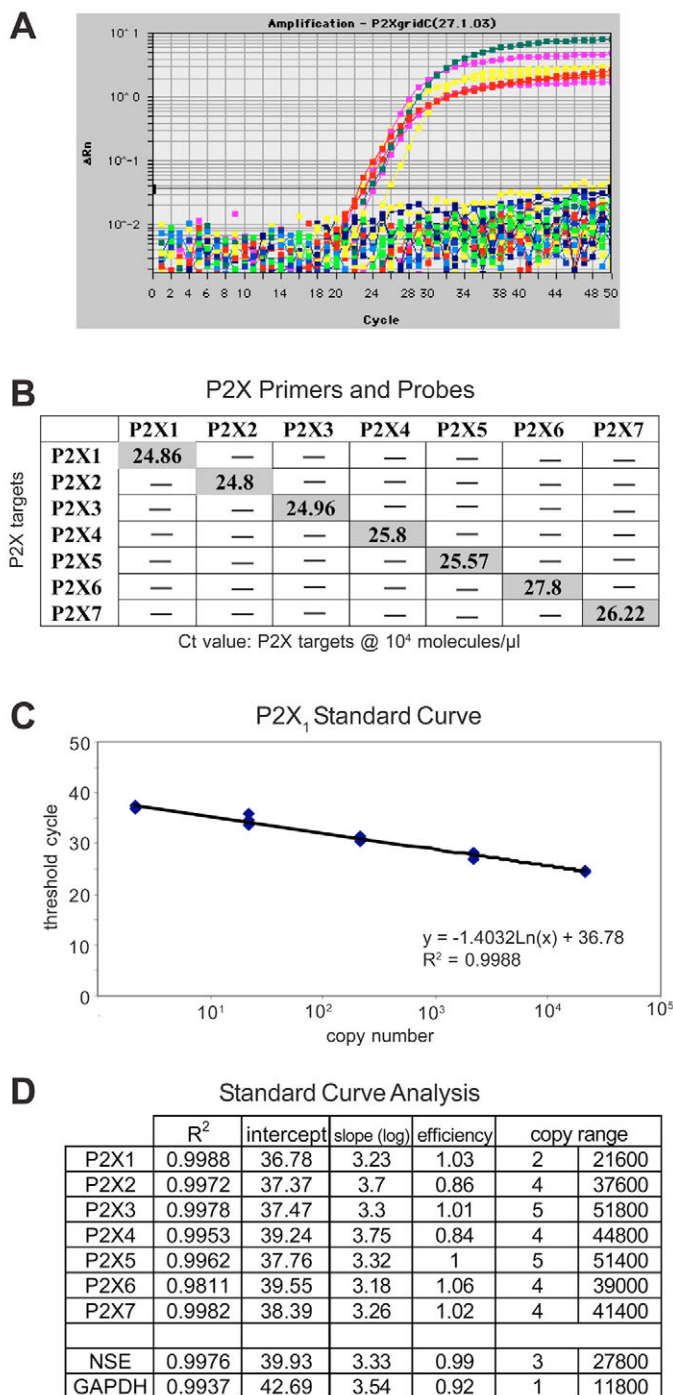|	R^2	intercept	slope (log)	efficiency	copy range	
P2X1	0.9988	36.78	3.23	1.03	2	21600
P2X2	0.9972	37.37	3.7	0.86	4	37600
P2X3	0.9978	37.47	3.3	1.01	5	51800
P2X4	0.9953	39.24	3.75	0.84	4	44800
P2X5	0.9962	37.76	3.32	1	5	51400
P2X6	0.9811	39.55	3.18	1.06	4	39000
P2X7	0.9982	38.39	3.26	1.02	4	41400
NSE	0.9976	39.93	3.33	0.99	3	27800
GAPDH	0.9937	42.69	3.54	0.92	1	11800

Fig. 2. Specificity of P2X primer and probe sets and standard curve analysis. (**A**) Real-time PCR amplification plot showing specificity of P2X receptor primer/probe sets with their target templates. Seven successful amplifications are shown, with absence of amplification of mismatched templates (see B). (**B**) Grid representation of primer and probe specificity showing C_T values for on-target cDNA amplification for all seven P2X receptors. Note the absence of non-specific amplification. (**C**) An example of a standard curve for P2X$_1$ receptor cDNA amplification. Note the linearity to <10 copies. (**D**) Standard curve analysis of the P2X receptor targets showing linearity of all seven dilution series. GAPDH, glyceraldehyde-3-phosphate dehydrogenase; NSE, neuron-specific enolase. Copy range used for the standard curves is estimated from the serial dilutions of template cDNAs.

obtained by confocal microscopy (TSCD4D; Leica, Germany). TIFF-format images were processed through Adobe Photoshop (v.6.0; Adobe Systems, San Jose, CA). Confocal images were restored to grayscale and optimized for contrast. P2X$_3$ polyclonal rabbit antiserum (Neuromics, Bloomington, MN) was targeted to residues 383-397 (VEKQSTDSGAYSIGH), P2X$_4$ polyclonal rabbit antiserum (Alomone Laboratories, Israel) was targeted to residues 370-388 (YVEDYEQGLSGEMNQ), and P2X$_2$ was targeted to residues 96-113 (VSIITRIEVTPSQTLGTC) (Kanjhan et al., 1996). Antibody specificity was confirmed by omission of the primary antibody and by pre-adsorption of the primary antibody with the target peptide.

Expression of the recombinant P2X$_{2-3/3}$ receptor
DNA constructs
The P2X$_{2-3}$ receptor cDNA was prepared by substituting an *Nde*1-*Eco*R1 DNA fragment from full-length P2X$_{2-1}$ with an *Nde*1-*Eco*R1 DNA fragment from a PCR 2.1 TA clone containing a 600-bp PCR product of the P2X$_{2-3}$ variant obtained by RT-PCR from cochlear tissue. The rat P2X$_3$ receptor cDNA was provided by our University College London collaborators. Full-length cDNAs for P2X$_{2-3}$ and P2X$_3$ were ligated into the mammalian expression vector pcDNA3.1 (Invitrogen) using *Bam*H1-*Eco*R1 and *Hind*111-*Eco*R1 sites, respectively. Plasmids were linearized with *Eco*RV for P2X$_{2-3}$ and *Eco*R1 for P2X$_3$ and cRNA synthesis was directed by T7 RNA polymerase (CapScribe; Roche). Oocytes were harvested from anesthetized *Xenopus laevis* frogs and defolliculated as previously described (Wildman et al., 2002). P2X$_{2-3}$ and P2X$_3$ cRNAs were co-injected into defolliculated *Xenopus* oocytes using a 1:2 ratio. Oocytes were incubated at 18°C for 48 hours and then analyzed using two-electrode voltage-clamp recording.

Voltage clamp of *Xenopus* oocytes
Agonist-activated membrane currents were recorded from oocytes injected with P2X receptor cRNAs using a two-electrode voltage-clamp amplifier (Axoclamp 2A; Axon Instruments, Union City, CA). The voltage and current electrodes were filled with 3.0 M KCl. Oocytes were superfused with Ringer's solution (pH 7.5) (containing 110 mM NaCl, 2.5 mM KCl, 1.8 mM CaCl$_2$ and 5 mM HEPES). Agonists were prepared in normal Ringer's solution and superfused (12 ml/minute) by a gravity-fed continuous flow system allowing rapid addition and washout of compounds. Agonists were added until peak current response was reached and then washed out for 20 minutes. Data for concentration-response curves were normalized to the maximum current (I_{max}) evoked by ATP (100 μM). Data are presented as the mean±s.e.m. of three or more datasets using different oocytes. Concentration-response curves and inhibition curves were fitted by non-linear regression analysis (Prism v2.0, GraphPad).

Drugs
ATP and related nucleotides were obtained from Sigma-Aldrich and TNP-ATP from Molecular Probes (Eugene, OR). All reagents were AnalaR grade from Sigma-Aldrich.

Patch clamp of SGN
Whole-cell voltage-clamp of the SGN in situ in the cochlear slices was performed as described in our previous pharmacological characterization of these neurons (Salih et al., 2002). Gigaseal recordings were obtained using micropipettes with a mean input resistance of ~1.5 mOhms. The recording electrodes were filled with 140 mM KCl, 10 mM NaCl, 2 mM MgCl$_2$, 5 mM HEPES, 5 mM EGTA and 10 mM glucose. ATP and associated agonists and antagonists were bath- or pressure-applied through a micropipette with the SGN voltage-clamped at –60 mV. Currents were recorded with PClamp6 software and an Axopatch 200B patch amplifier, low-pass filtered at 1-5 kHz and digitized at 5-20 kHz with a DigiData 1200 series interface (Axon Instruments, Foster City, CA). Voltage errors caused by series resistance were compensated at 70-90% online, and residual errors corrected during analysis. Junction potentials were compensated during analysis. Data are presented as mean±s.e.m.

Spiral ganglion explants
P4 rat spiral ganglion explants were cultured as previously described (Aletsee et al., 2003). The explants were placed into tissue culture in 24-well plates (Costar) for three days using Dulbecco's modified Eagle's medium (DMEM; Invitrogen), with N-2 supplement (Invitrogen), 25 mM

HEPES, 4.5 mg/ml glucose and 30 U/ml penicillin. The media was supplemented with BDNF (1 or 10 ng/ml; UpState) with or without ATPγS (100 μM; Sigma) or α,βMeATP (100 μM; Sigma). Media was changed daily. The explants were fixed with paraformaldehyde (4% in 0.1 M PBS, pH 7.3) and then immunostained for neurofilament (1:500 rabbit anti-neurofilament, 200 IgG; Sigma no. N4142), with an FITC-conjugated donkey anti-rabbit IgG (1:100; Jackson ImmunoResearch no. 711-095-152) secondary antibody. Neurites were evaluated from digital epifluorescence images of each explant obtained using the Spot imaging system (RT-color model 2.2.1 camera; Spot v.4.6 software; Diagnostic Instruments, USA). This includes a tracing algorithm for determining the length and number of neurites. Neurites were traced from their point of exit from the explant to their termination. All of the neurites on each explant were traced, along their entire length. The program computed the length of each traced neurite as the sum of vector lengths along the trace. Numbers were determined as a count of the separate traces performed on each explant image. Data were analyzed by ANOVA and Fisher's post-hoc test, with Bonferroni correction for multiple tests.

RESULTS

P2X$_3$ and P2X$_2$ are the dominant ATP-gated ion channel subunits expressed by individual neonatal SGN

P2X receptor-activated membrane currents were recorded under voltage-clamp (V_H=–60 mV) from a subset of neonatal (P2-P4) rat SGN (n=16) to confirm their phenotype prior to extraction of the cytoplasm for RT-PCR analysis. The cells had inward current responses to focally applied ATP and α,βMeATP, a P2X$_3$- and P2X$_{2/3}$-selective agonist [mean=–727±88 pA (n=9) and –350±127 pA (n=7), respectively; Fig. 3A-C], consistent with our previous detailed pharmacological analysis of these neurons (Salih et al., 2002). Five neonatal rat SGN were examined for P2X$_{2/3}$ heteromeric assembly using the selective antagonist A-317491 [500 nM, after Jarvis et al. (Jarvis et al., 2002)]. Inward current responses to focal application of ATP (100 μM, 5 seconds) averaged –354±71.1 pA. Application of ATP in the presence of A-317491 produced a 47.2±7.5% block of the ATP response (P=0.019, Student's paired t-test; Fig. 3C). Recovery from the block averaged 35% after 10 minutes of antagonist washout.

The relative abundance of all seven P2X receptor transcripts was determined in SGN using single-cell real-time RT-PCR. Cytoplasm of individual SGN from the cochlear slices was aspirated into glass micropipettes. The single-cell mRNA sample was reverse transcribed into cDNA and divided into samples that provided a template for analysis of the seven P2X receptors and positive control genes. Fig. 3D shows examples of single-cell real-time PCR amplification plots from cells analyzed for P2X$_3$ cDNA. The C_T values assigned for each neuron sample ranged between 34 and 38 cycles, corresponding to between 3 and 159 P2X$_3$ cDNA molecules based on calibration curves run in tandem (see Materials and Methods). In a sample of 48 individual neurons, there was a clear difference in transcript levels across the seven P2X receptor subunits (P<0.0001; one-way ANOVA). P2X$_3$ and P2X$_2$ were the most prevalent cDNAs; P2X$_3$ averaged approximately twice the number of transcript copies (mean=48±9 copies per cell) compared with P2X$_2$ (mean=25±5) (P=0.004; Student's paired t-test) (Fig. 3E). The mean P2X$_4$ transcript copy number detected was 17±4. The remaining P2X subunit mRNAs were detected at between two and five copies per cell (Fig. 3E). P2X$_2$, P2X$_3$ and P2X$_4$ transcripts were detected in most neurons [37/48 (77%), 41/48 (85%) and 40/48 (83%), respectively], whereas the detection frequency of the other P2X subtypes ranged from 17-27%. Fig. 3F shows the normalized copy number for each of the seven P2X receptor subunit

isoforms expressed by individual neurons, demonstrating the dominance of the P2X$_2$ and P2X$_3$ transcripts. As a control for specificity of this single-cell gene quantification assay, transcript numbers of the housekeeping genes *Gapdh* and *Nse* were also assessed and the mRNA abundance of these targets was comparable to P2X transcript levels (Fig. 3E). The mean transcript numbers of 62±16 for *Gapdh* and 11±3 for *Nse* were in keeping with the expected range for housekeeping genes (Warrington et al., 2000). Samples taken from bath solution and the no-template controls remained clear for the full 50 PCR cycles. No signal was obtained from neuron samples when reverse transcription was omitted (–RT control, n=5).

The relatively higher expression of P2X$_2$ and P2X$_3$ mRNAs in the SGN was compatible with multimeric P2X receptor subunit assembly. Confocal immunofluorescence (Fig. 3G) confirmed the localization of P2X$_2$ and P2X$_3$ protein to the plasma membrane of the spiral ganglion cell bodies, as shown previously by our group (Huang et al., 2005; Järlebark et al., 2000). By contrast, P2X$_4$ immunolabeling of the spiral ganglion was considerably weaker, with diffuse signal in the soma of the SGN (Fig. 3G). When considered alongside the single-cell real-time RT-PCR analysis, these data indicate the likely dominance of an ATP-gated ion channel assembled with a P2X$_3$:P2X$_2$:P2X$_3$ subunit stoichiometry, as reported in a recombinant expression model (Jiang et al., 2003). However, the unique pharmacology of the SGN (Salih et al., 2002) is incompatible with the properties of the recombinant P2X$_{2-1}$/P2X$_3$/P2X$_3$ heteromer (Jiang et al., 2003; Liu et al., 2001), particularly with regard to agonist profile and desensitization rate. Given the prevalence of alternative splicing of the *P2X$_2$* (also known as *P2rx2*) gene in the SGN (Salih et al., 1998), the potential contribution of such splicing to the putative SGN P2X$_{2/3}$ heteromer was investigated.

P2X$_{2-3}$ splice variant is the dominant P2X$_2$ isoform expressed in neonatal SGN

We have previously shown that SGN of adult rat cochlea express mRNA for three P2X$_2$ splice variants (Salih et al., 1998), two of which, P2X$_{2-1}$ (Brake et al., 1994) and P2X$_{2-2}$ (Brändle et al., 1997), have widespread distribution in other tissues and have been characterized utilizing heterologous expression systems. The third isoform, P2X$_{2-3}$ (Salih et al., 1998), has a 39-bp deletion adjacent to the carboxy-terminus coding region (13 amino acid truncation). A schematic showing P2X$_{2-3}$ compared with the other two isoforms is presented in Fig. 4A. The expression profile for these three P2X$_2$ transcripts in SGN of neonatal cochleae was determined by end-point single-cell RT-PCR. Fig. 4B shows the predominance of the P2X$_{2-3}$ splice variant. In a sample of 31 neurons, P2X$_{2-3}$ had the highest detection frequency (74%), and most commonly, was the only P2X$_2$ isoform detected (Fig. 4C). This suggests that the P2X$_{2-3}$ splice variant is the most likely P2X$_2$ isoform within a putative SGN P2X$_{2-3}$/P2X$_3$/P2X$_3$ heteromer, henceforth referred to as the P2X$_{2-3/3}$ receptor.

Functional characterization of the P2X$_{2-3/3}$ receptor

The P2X$_{2-3/3}$ receptor was functionally characterized in the *Xenopus* oocyte expression system to determine its likely candidacy as the native neonatal rat SGN P2X receptor. Initial experiments confirmed the functionality of the P2X$_{2-3}$ subunit as a homomer (Table 3; D.G. and G.D.H., unpublished). Notable characteristics included an EC$_{50}$ of 9 μM, and selective activation by ATP and 2MeSATP, but not α,βMeATP. Based on the relative abundance of P2X transcripts

determined by real-time RT-PCR, P2X$_{2-3}$ and P2X$_3$ cRNAs where then co-injected into *Xenopus* oocytes in a 1:2 ratio. The resulting P2X$_{2-3/3}$ receptor showed an extended agonist sensitivity to include α,β-meATP and ADP (Fig. 5A). This profile does not match the previously characterized recombinant P2X$_{2-1/3}$ receptor (Liu et al., 2001), as shown by its sensitivity to 2MeSATP and ADP. In addition, this novel P2X$_{2-3/3}$ heteromer also had greater sensitivity to ATP (EC$_{50}$=0.4 μM at pH 7.5) than the P2X$_{2-1/3}$ heteromer (Fig. 5B; Table 3). At pH 6.5, the P2X$_{2-3/3}$ receptor exhibited enhanced sensitivity to

ATP because of positive allosteric modulation by protons, as previously reported for P2X$_{2-1}$ homomers (Kanjhan et al., 2003; King et al., 1996; Stoop et al., 1997). This positive allosteric modulation of the ATP response is pronounced in the native SGN (Salih et al., 2002). Furthermore, the antagonist trinitrophenyl ATP (TNP-ATP) inhibited the recombinant P2X$_{2-3/3}$ receptor (IC$_{50}$=3.5 μM) similar to the SGN. The correlation in phenotype between the recombinant P2X$_{2-3/3}$ receptor and the properties of the P2X receptor in the neonatal rat SGN is summarized in Table 3.
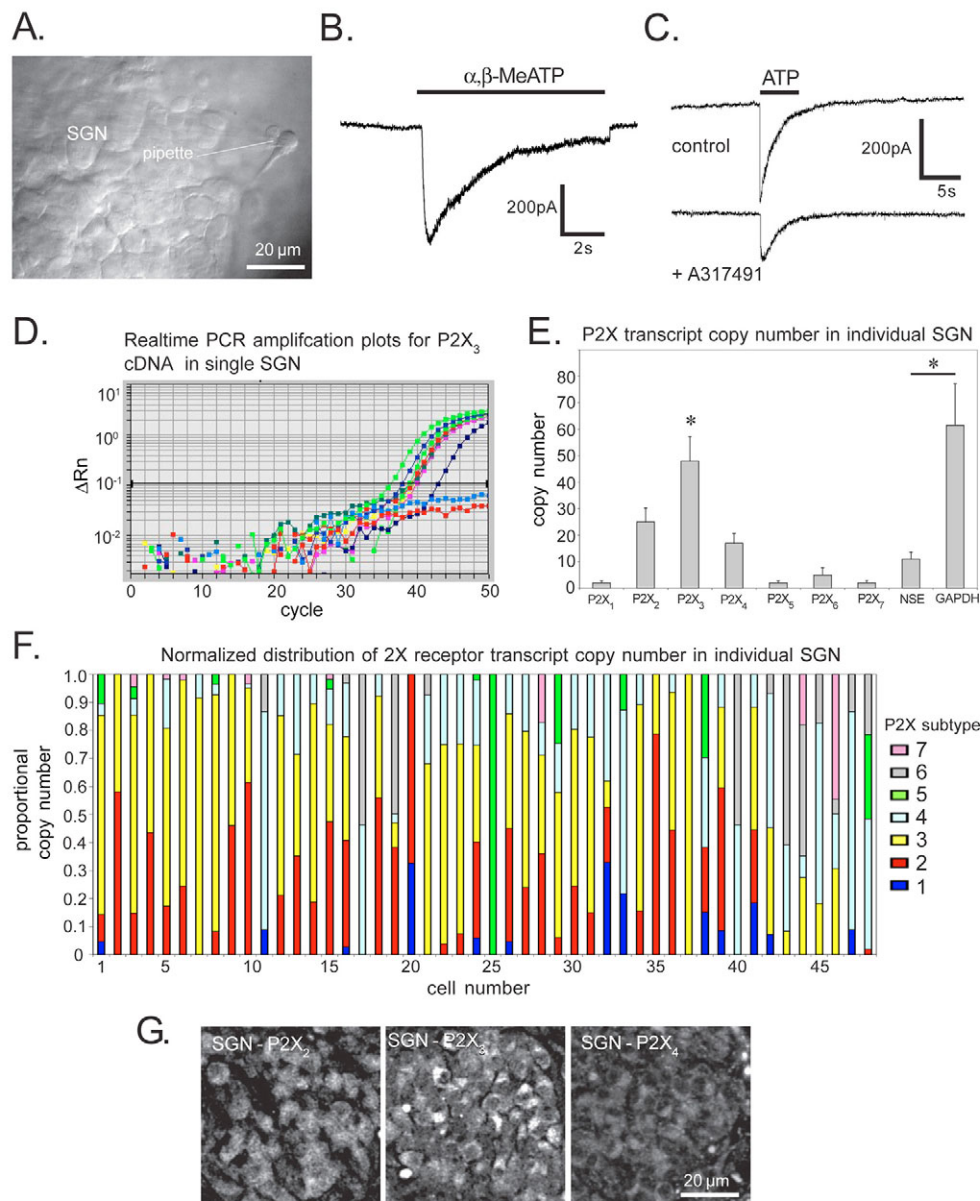

Fig. 3. Analysis of P2X receptor expression in neonatal rat SGN. (**A**) Isolation of a single SGN from a P4 rat cochlear slice using a micropipette. (**B**) Example of an inward current response to the P2X$_3$ and P2X$_{2/3}$ receptor agonist α,βMeATP (100 μM) in a SGN using whole-cell voltage clamp (holding potential –60 mV). (**C**) Block of the ATP response (100 μM, 5 seconds of focal application) by the P2X$_{2/3}$ receptor-specific antagonist A-317491 (500 nM, bath superfusion). (**D**) Real-time PCR amplification plot showing detection of P2X$_3$ cDNA in a sample of individual SGN. (**E**) Average transcript copy number for each P2X receptor subunit and the housekeeping genes *Nse* and *Gapdh* in individual neurons. Note that the P2X$_3$ transcript number was twice that of P2X$_2$ (*P<0.01; P2X$_3$ transcript number was significantly greater than the other P2X subunits; GAPDH transcript copy number was significantly greater than NSE transcript copy number). (**F**) Relative distribution of P2X receptor subunits in the population of SGN. This plot shows the normalized mRNA transcript copy number for each of the seven candidate P2X receptor subunits expressed by individual SGN. (**G**) Immunofluorescence labeling of P2X$_2$, P2X$_3$ and P2X$_4$ in neonatal (P4) spiral ganglion tissue.
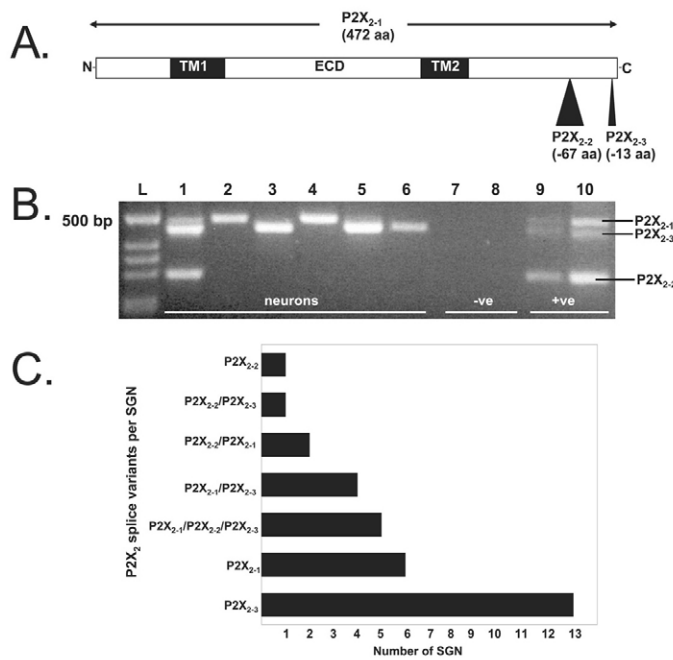
Fig. 4. Variation in expression of P2X$_2$ splice variants in SGN.
(**A**) Schematic of the three P2X$_2$ isoforms expressed in SGN, showing their C-terminal region variation. ECD, extracellular domain; TM, transmembrane domain. (**B**) End-point single-cell RT-PCR analysis of a sample of six SGN showing the expression of P2X$_2$ isoforms in individual cells (lanes 1-6). Amplicon sizes: P2X$_{2-1}$=499 bp; P2X$_{2-2}$=292 bp; P2X$_{2-3}$=480 bp. P2X$_{2-3}$ was the most prominent isoform (4/6 cells). The agarose gel also includes two positive controls of cDNA from whole spiral ganglion (lane 9) and whole cochlea (lane 10). Lane 7 (–) control for no template. Lane 8 (–) bath sample processed for RT-PCR. (**C**) Analysis of P2X$_2$ splice variant combinations detected in the 31 single-cell RT-PCR experiments. P2X$_{2-3}$ was the dominant isoform either expressed alone or with one or more of the other isoforms (23/31 neurons).
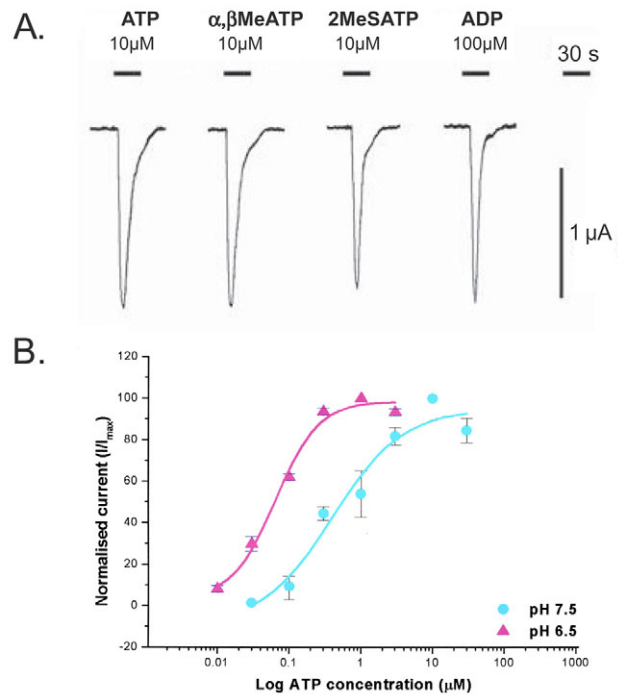

Fig. 5. Pharmacology of the recombinant P2X$_{2-3/3}$ receptor.
(**A**) Injection of P2X$_{2-3}$ and P2X$_3$ mRNAs in a ratio of 1:2 into *Xenopus* oocytes resulted in expression of ATP-gated inward currents with a broad sensitivity to ATP agonists. (**B**) Concentration-response curves for ATP at pH 7.5 show an EC$_{50}$ of 0.4 μM for these ATP-gated ion channels. Acidification to pH 6.5 produced a leftward shift in the concentration-response curve, to reduce activation thresholds to <10 nM ATP. This is attributable to positive allosteric modulation by protons acting through the P2X$_2$ subunit.

Expression of P2X receptor mRNAs in rat spiral ganglion during postnatal development

To establish the likely temporal expression profile for the P2X$_{2-3/3}$ receptor, end-point RT-PCR was performed using total RNA isolated from rat spiral ganglion tissue at postnatal ages P0-P14 (Fig. 6). This spanned the period of afferent neurite reorganization in the cochlea. These data demonstrated that at P0, all seven P2X transcripts were present. However, the P2X$_1$ transcript diminished after P0. P2X$_3$ and P2X$_5$ transcripts were downregulated by P14. Expression of P2X$_2$, P2X$_4$, P2X$_6$ and P2X$_7$ transcripts was detected at all ages. These

findings provide a consolidation of analysis of P2X receptor expression in the developing rat spiral ganglion, and is supported by several preceding studies (Brändle et al., 1999; Housley et al., 1998; Järlebark et al., 2000; Nikolic et al., 2001; Nikolic et al., 2003; Salih et al., 1998). These data are compatible with our earlier analysis of P2X$_3$ receptor expression in the rat and mouse that demonstrated coincident gene transcription and protein translation (Huang et al., 2005; Huang et al., 2006). The downregulation of P2X$_3$ by P14 indicates that the putative P2X$_{2-3/3}$ receptor is specific to the period of neurite development.

Table 3. Phenotype of the P2X$_{2-3/3}$ receptor expressed in *Xenopus* oocytes compared with the spiral ganglion neuron P2X receptor and other recombinant P2X receptor isoforms

	P2X$_{2-3/3}$*	SGN[†]	P2X$_{2-1/3}$[‡]	P2X$_{2-1}$[§,¶,**]	P2X$_{2-3}$[††]	P2X$_3$[¶,‡‡]
α,βmeATP	+	+	+	–	–	+
2meSATP	+	+	–	+	+	+
ADP	+	+	–	–	–	+
Desensitization	Fast (5 seconds)	Fast (2 seconds)	Slow	Slow	Slow	Very fast (100 mseconds)
ATP (EC$_{50}$)	0.45 μM	18 μM	1 μM	1-62 μM[§§]	9 μM	1 μM
Protons	Potentiate	Potentiate	Potentiate	Potentiate	Potentiate	Inhibit
TNP-ATP (IC$_{50}$)	3.5 μM	407 nM	4 nM	1 μM	nd	1 nM

*This study; [†]Salih et al., 2002; [‡]Lewis et al., 1995; [§]Brake et al., 1994, King et al., 1996, Khakh et al., 2001; [¶]North, 2002; [**]Kanjhan et al., 2003; [††]D.G. et al., unpublished; [‡‡]Chen et al., 1995; [§§]EC50 reported for ATP at P2X2 receptors is variable (see §,¶,**). +, response; –, no response; nd, not determined.
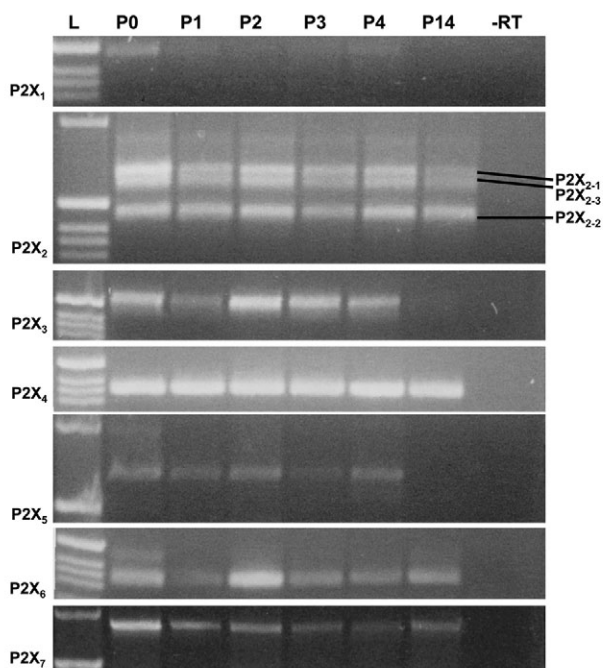
Fig. 6. Developmental profile of P2X receptor subunit expression in rat spiral ganglion tissue from P0-P14, determined by end-point RT-PCR. Note the downregulation of the $P2X_3$ transcript by P14.

Purinergic inhibition of BDNF-dependent spiral ganglion neurite growth

The functional significance of the $P2X_{2-3/3}$ receptor on neurite growth was investigated in a neonatal rat spiral ganglion explant model. Explants from P4 rat spiral ganglia were cultured for 72 hours in the presence of BDNF (Brors et al., 2002) with and without the P2X receptor agonists $ATP\gamma S$ and $\alpha,\beta MeATP$ (100 μM). BDNF (10 ng/ml) promoted SGN neurite extension by 57% ($P<0.05$, $n=11$; Student's unpaired t-test) and increased the neurite number by 51% ($P<0.01$) (compare Fig. 7D with Fig. 7A,G-J). The neurotrophic action provided by BDNF was dose-dependent, with no significant effect at 1 ng/ml (Fig. 7G,H). The ATP analogs, while having no independent effect ($P>0.05$; compare Fig. 7B,C with Fig. 7A,G-J), strongly inhibited the BDNF-dependent (10 ng/ml) trophic action on neurite growth and development. $ATP\gamma S$ eliminated the BDNF-dependent neurite extension ($P<0.001$; Fig. 7E,G) and reduced the BDNF-dependent increase in neurite number by ~50% ($P<0.05$; compare Fig. 7D with Fig. 7E,H). $\alpha,\beta MeATP$ reduced the BDNF-dependent neurite extension by 27% ($P=0.002$; compare Fig. 7D with Fig. 7F,I) and number by 21% (Fig. 7F,J). These data demonstrate a purinergic inhibitory control of BDNF-dependent neurotrophism in the spiral ganglion invoked by putative $P2X_{2-3/3}$ receptor activation.

DISCUSSION

Reorganization of synaptic contacts between the primary auditory neurons and the sensory hair cells of the developing rat cochlea is required to ensure that the type I fibers exclusively innervate IHC, while the neurites from the type II SGN innervate the OHC. This requires withdrawal of the type I fibers from the OHC, and pruning of their synapses with IHC, a process that is largely resolved in the first postnatal week in the rat cochlea (for a review, see Rubel and Fritzsch, 2002). Here we show that coincident with this period, there is tight gene regulation of the $P2X_3$ subunit and a bias towards the

$P2X_{2-3}$ subunit splice variant. The match of phenotype of the recombinant $P2X_{2-3/3}$ receptor with that of the native SGN P2X receptor membrane-current properties indicates that this is the principal P2X receptor type in the SGN over this crucial period for neurite reorganization in the cochlea. The effect of the activation of this receptor type by the $P2X_{2/3}$ receptor agonists $ATP\gamma S$ and $\alpha,\beta MeATP$ leads to potent inhibition of the extension and branching of the SGN. These data suggest that the molecular signaling, which leads to withdrawal of neurites from inappropriate targets, may involve the release of extracellular ATP, which, acting through the $P2X_{2-3/3}$ receptor, diminishes the neurotrophic signaling between the hair cells and the SGN neurites.

As noted, P2X receptors are ATP-gated ion channels with a trimeric subunit configuration (Nicke et al., 1998), which, in the case of $P2X_3/P2X_2/P2X_3$ heteromers, incorporates one $P2X_2$ subunit and two $P2X_3$ subunits (Jiang et al., 2003). Khakh and Egan recently showed that these P2X-subunit trimers form a functional non-selective cation channel by utilizing both membrane-spanning domains of each subunit to line the channel pore (Khakh and Egan, 2005). Our study shows for the first time that $P2X_2$ and $P2X_3$ (also known as $P2rx3$) gene expression within individual neurons is coregulated so that transcript levels predispose the subsequent assembly of the translated proteins in the appropriate stoichiometry. An additional level of P2X receptor gene regulation has also been revealed in specificity of $P2X_2$ receptor mRNA splicing. It is likely that the majority of SGN neurons analyzed in this study were type I, given their preponderance; however, we have previously demonstrated that type I and type II SGN express comparable ATP-gated currents (Jagger and Housley, 2003) and both inner radial fibers (type I) and outer spiral fibers (type II) are immunopositive for $P2X_2$ and $P2X_3$. Although ATP-release from the organ of Corti has been confirmed (Wangemann, 1996), the source of this P2X receptor agonist remains unknown, but may include hair cells, given the corelease of ATP with other transmitters such as glutamate (Burnstock, 2004). Thus, it is likely that the $P2X_{2-3/3}$ receptor-mediated regulation of neurite development demonstrated here would apply to both types of SGN.

Our single-cell real-time RT-PCR study resolved significant differences in transcript copy number between the seven different P2X subunits and also between the two housekeeping genes $Gapdh$ and Nse. The mRNA abundance for these genes ranged from <10 to hundreds of copies. This is a relative transcript measurement, detecting a proportion of mRNAs available from each neuron. The remarkable feature of the molecular analysis provided by the TaqMan-based RT-PCR is that between-sample variation is sufficiently small to enable statistically significant discrimination when single-cell transcript copy numbers vary by tens of copies (Fig. 3E). The single-cell transcript levels were comparable to those previously described for other ion channel subunits (Sucher et al., 2000) and for transcription factors and housekeeping genes (Wagatsuma et al., 2005; Warrington et al., 2000). Our application of TaqMan-based real-time PCR in single cells is also supported by recent investigations of dopaminergic receptor mRNA transcript levels (Liss et al., 2001), mGluR in rod photoreceptors (Kamphuis et al., 2003) and 5HT receptors in hypoglossal motoneurons (Zhan et al., 2002). These studies, alongside critical reviews of quantitative RT-PCR technology (Bustin, 2002; Fink et al., 1998; Ginzinger, 2002; Pfaffl et al., 2002; Wagatsuma et al., 2005), establish criteria for determining the validity of quantifying transcripts at low copy number. The key requirements are to confirm amplicon specificity, PCR efficiency and detection sensitivity. In the present study, possible amplification of genomic targets was precluded by the
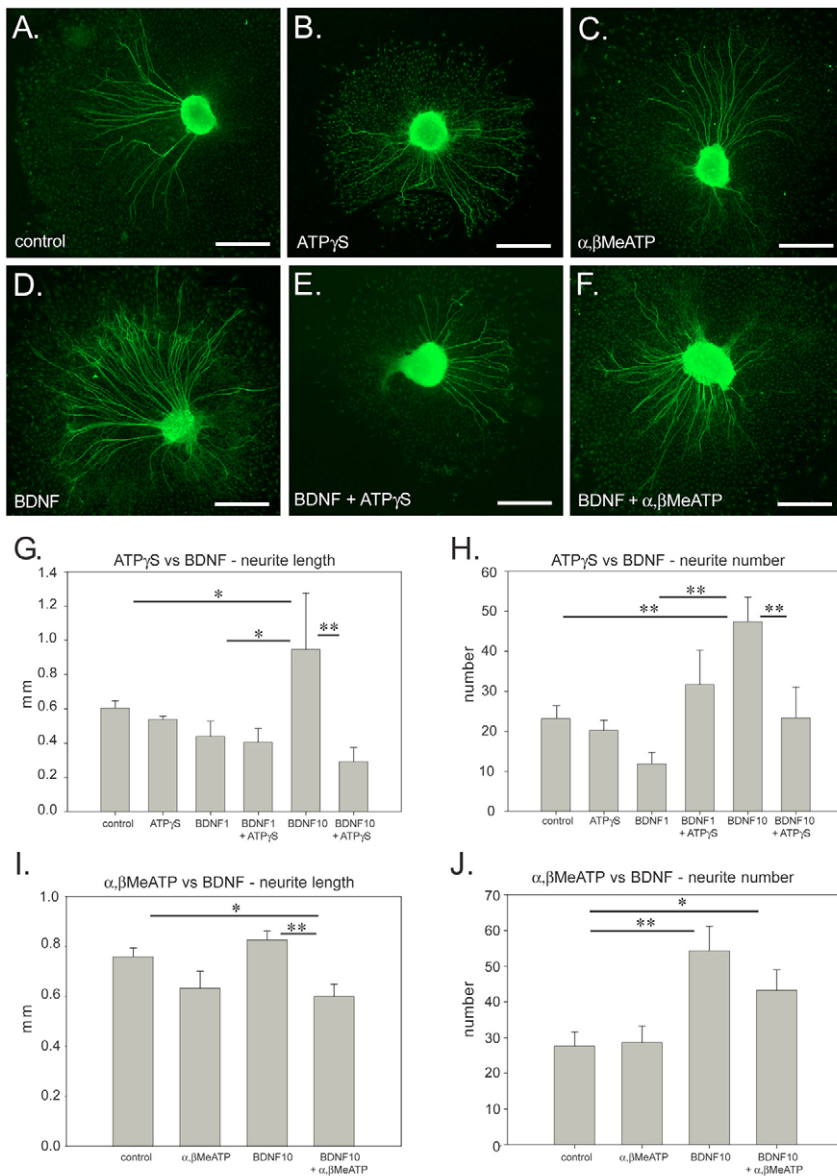
Fig. 7. Purinergic receptor antagonism of BDNF-dependent spiral ganglion neurite development. Cultures of P4 spiral ganglion explants were treated for three days with medium (control) or with addition of BDNF at 1 ng/ml or 10 ng/ml. The effect of P2X receptor activation on BDNF-dependent neurite development was assessed with ATPγS (100 μM) and α,βMeATP (100 μM). (**A-F**) Immunofluorescence images of spiral ganglion explants labeled for neurofilament. BDNF at 10 ng/ml. Scale bars: 500 μm. (**G,H**) Experiments comparing BDNF-induced neurite growth with and without ATPγS (n=12-20 explants per group). (**I,J**) Experiments comparing BDNF-induced neurite growth with and without α,βMeATP (n=12 explants per group). *P<0.05; **P<0.01.

absence of amplicons from –RT controls. In addition, the separation of the single-cell template into 10 samples effectively eliminated potential genomic DNA targets (Johansen et al., 1995). Amplification of cDNA templates derived from sources other than individual SGN were deemed unlikely, based on the lack of amplification of no-template controls, including perfusion media.

Our data suggest that in the early postnatal SGN, the $P2X_{2-3}$ subunit is the preferentially expressed $P2X_2$ variant. This isoform has a 39-bp deletion resulting in a loss of 13 amino acids immediately before the cytosolic carboxy terminus (Salih et al., 1998). The identification of functionality of this PX_{2-3} splice variant within a $P2X_{2/3}$ heteromeric receptor complex provides further insight into the contribution of the C-terminal domain of these subunits as a regulator of agonist profile, receptor desensitization and subunit interaction in P2X receptors (for a review, see Khakh and North, 2006). The recombinant $P2X_{2-3}$ homomer had many similarities with the $P2X_{2-1}$ homomeric receptor (Brake et al., 1994) (Table 3), however, the $P2X_{2-3/3}$ heteromer produced significant changes in receptor phenotype from that reported for the $P2X_{2-1/3}$ receptor (Lewis et al., 1995), including faster desensitization, and de

novo sensitivity to 2MeSATP and ADP. Studies of the other functional variant in rat, $P2X_{2-2}$ (Brändle et al., 1997), as well as engineered C-terminal region variants, demonstrate influences on trafficking of the subunits, interaction with other receptor subunits, desensitization rate and ion permeability (Brändle et al., 1997; Chaumont et al., 2004; Eickhorst et al., 2002; Gendreau et al., 2003).

Evidence is emerging that P2X receptor-based signaling has neurotrophic actions. In several neuronal culture models, activation of P2X receptors complements neurotrophin activity. For example, in PC12 cells, enhanced neurite initiation is induced by application of ATP and ATPγS, at suboptimal nerve growth factor (NGF) levels (D'Ambrosi et al., 2001). NGF and ATP induced an upregulation of several P2X receptors, including $P2X_2$, $P2X_3$ and $P2X_4$. Given that P2X receptors have the highest Ca^{2+} permeability of transmitter-gated cation channels (Egan and Khakh, 2004), it is likely that ATP, acting as a transmitter, or paracrine signaling factor has a neurotrophic action through Ca^{2+} signaling (Hegarty et al., 1997). P2X receptors are also likely to complement neurotransmitter signaling elements such as glutamate and acetylcholine (Fu, 1995; Gu and MacDermott, 1997; Jo and Schlichter, 1999) to engage

neurotrophic mechanisms, such as the stabilization of synapses. P2X receptors may exert conflicting influences on neural growth. In a neural tube explant model, P2X$_3$ receptors, activated by α,βMeATP, have been implicated in the inhibition of motor axon outgrowth during embryonic neurogenesis, affecting both neurite length and number (Cheung et al., 2005). The influence of P2X$_3$ receptor signaling on embryonic neurogenesis in the CNS is supported by the wide distribution of this receptor during development of the CNS, with rapid downregulation in the postnatal period (Cheung and Burnstock, 2002).

In the developing cochlea, neurite growth is supported by both BDNF-TrkB and NT3-TrkC signaling pathways. Evidence suggests that release of these neurotrophins from the sensorineural tissue, including the hair cells, supports SGN development. In explant models, SGN extension and branching is greatly enhanced by treatment with these neurotrophins (Aletsee et al., 2001; McGuinness and Shepherd, 2005; Ryan et al., 2006). Our data, showing the ATPγS and α,βMe ATP-inhibition of SGN neurite development induced by BDNF, strongly supports a role for the P2X receptors in the regulation of neurite-hair cell trophism. Developmental regulation of P2X$_3$ receptor expression to the period when the neurites are reorientated into the mature configuration, and a bias towards P2X$_{2-3}$ expression, all combine to suggest that ATP provides a signal through a specific P2X receptor – P2X$_{2-3/3}$. This novel receptor acts to inhibit BDNF neurotrophism and may provide the signal that induces disengagement of synaptic connections in the early postnatal rat cochlea, as a prelude to the final neural differentiation required for functional auditory neurotransmission.

References

Aletsee, C., Beros, A., Mullen, L., Palacios, S., Pak, K., Dazert, S. and Ryan, A. F. (2001). Ras/MEK but not p38 signaling mediates NT-3-induced neurite extension from spiral ganglion neurons. *J. Assoc. Res. Otolaryngol.* **2**, 377-387.

Aletsee, C., Brors, D., Milynski, R., Ryan, A. F. and Dazert, S. (2003). Branching of spiral ganglion neurites is induced by focal application of fibroblast growth factor-1. *Laryngoscope* **113**, 791-796.

Berglund, A. M. and Ryugo, D. K. (1987). Hair cell innervation by spiral ganglion neurons in the mouse. *J. Comp. Neurol.* **255**, 560-570.

Brake, A. J., Wagenbach, M. J. and Julius, D. (1994). New structural motif for ligand-gated ion channels defined by an ionotropic ATP receptor. *Nature* **371**, 519-523.

Brändle, U., Spielmanns, P., Osteroth, R., Sim, J., Surprenant, A., Buell, G., Ruppersberg, J. P., Plinkert, P. K., Zenner, H. P. and Glowatzki, E. (1997). Desensitization of the P2X$_2$ receptor controlled by alternative splicing. *FEBS Lett.* **404**, 294-298.

Brändle, U., Zenner, H. P. and Ruppersberg, J. P. (1999). Gene expression of P2X-receptors in the developing inner ear of the rat. *Neurosci. Lett.* **273**, 105-108.

Brors, D., Aletsee, C., Schwager, K., Mlynski, R., Hansen, S., Schafers, M., Ryan, A. F. and Dazert, S. (2002). Interaction of spiral ganglion neuron processes with alloplastic materials in vitro(1). *Hear. Res.* **167**, 110-121.

Burnstock, G. (2004). Cotransmission. *Curr. Opin. Pharmacol.* **4**, 47-52.

Bustin, S. A. (2002). Quantification of mRNA using real-time reverse transcription PCR (RT-PCR): trends and problems. *J. Mol. Endocrinol.* **29**, 23-39.

Chaumont, S., Jiang, L. H., Penna, A., North, R. A. and Rassendren, F. (2004). Identification of a trafficking motif involved in the stabilization and polarization of P2X receptors. *J. Biol. Chem.* **279**, 29628-29638.

Chen, C. C., Akopian, A. N., Sivilotti, L., Colquhoun, D., Burnstock, G. and Wood, J. N. (1995). A P2X purinoceptor expressed by a subset of sensory neurons. *Nature* **377**, 428-431.

Cheung, K. K. and Burnstock, G. (2002). Localization of P2X$_3$ receptors and coexpression with P2X$_2$ receptors during rat embryonic neurogenesis. *J. Comp. Neurol.* **443**, 368-382.

Cheung, K. K., Chan, W. Y. and Burnstock, G. (2005). Expression of P2X purinoceptors during rat brain development and their inhibitory role on motor axon outgrowth in neural tube explant cultures. *Neuroscience* **133**, 937-945.

D'Ambrosi, N., Murra, B., Cavaliere, F., Amadio, S., Bernardi, G., Burnstock, G. and Volonte, C. (2001). Interaction between ATP and nerve growth factor signalling in the survival and neuritic outgrowth from PC12 cells. *Neuroscience* **108**, 527-534.

Egan, T. M. and Khakh, B. S. (2004). Contribution of calcium ions to P2X channel responses. *J. Neurosci.* **24**, 3413-3420.

Eickhorst, A. N., Berson, A., Cockayne, D., Lester, H. A. and Khakh, B. S. (2002). Control of P2X$_2$ channel permeability by the cytosolic domain. *J. Gen. Physiol.* **120**, 119-131.

Fink, L., Seeger, W., Ermert, L., Hanze, J., Stahl, U., Grimminger, F., Kummer, W. and Bohle, R. M. (1998). Real-time quantitative RT-PCR after laser-assisted cell picking. *Nat. Med.* **4**, 1329-1333.

Fu, W. M. (1995). Regulatory role of ATP at developing neuromuscular junctions. *Prog. Neurobiol.* **47**, 31-44.

Geal-Dor, M., Freeman, S., Li, G. and Sohmer, H. (1993). Development of hearing in neonatal rats: air and bone conducted ABR thresholds. *Hear. Res.* **69**, 236-242.

Gendreau, S., Schirmer, J. and Schmalzing, G. (2003). Identification of a tubulin binding motif on the P2X$_2$ receptor. *J. Chromatogr. B Analyt. Technol. Biomed. Life Sci.* **786**, 311-318.

Ginzinger, D. G. (2002). Gene quantification using real-time quantitative PCR: an emerging technology hits the mainstream. *Exp. Hematol.* **30**, 503-512.

Gu, J. G. and MacDermott, A. B. (1997). Activation of ATP P2X receptors elicits glutamate release from sensory neuron synapses. *Nature* **389**, 749-753.

Hegarty, J. L., Kay, A. R. and Green, S. H. (1997). Trophic support of cultured spiral ganglion neurons by depolarization exceeds and is additive with that by neurotrophins or cAMP and requires elevation of [Ca^{2+}]$_i$ within a set range. *J. Neurosci.* **17**, 1959-1970.

Housley, G. D., Luo, L. and Ryan, A. F. (1998). Localization of mRNA encoding the P2X$_2$ receptor subunit of the adenosine 5'-triphosphate-gated ion channel in the adult and developing rat inner ear by in situ hybridization. *J. Comp. Neurol.* **393**, 403-414.

Huang, L. C., Greenwood, D., Thorne, P. R. and Housley, G. D. (2005). Developmental regulation of neuron-specific P2X$_3$ receptor expression in the rat cochlea. *J. Comp. Neurol.* **484**, 133-143.

Huang, L. C., Ryan, A. F., Cockayne, D. A. and Housley, G. D. (2006). Developmentally regulated expression of the P2X$_3$ receptor in the mouse cochlea. *Histochem. Cell Biol.* **125**, 1-12.

Jagger, D. J. and Housley, G. D. (2003). Membrane properties of type II spiral ganglion neurones identified in a neonatal rat cochlear slice. *J. Physiol.* **552**, 525-533.

Jagger, D. J., Robertson, D. and Housley, G. D. (2000). A technique for slicing the rat cochlea around the onset of hearing. *J. Neurosci. Methods* **104**, 77-86.

Järlebark, L. E., Housley, G. D. and Thorne, P. R. (2000). Immunohistochemical localization of adenosine 5'-triphosphate-gated ion channel P2X$_2$ receptor subunits in adult and developing rat cochlea. *J. Comp. Neurol.* **421**, 289-301.

Jarvis, M. F., Burgard, E. C., McGaraughty, S., Honore, P., Lynch, K., Brennan, T. J., Subieta, A., Van Biesen, T., Cartmell, J., Bianchi, B. et al. (2002). A-317491, a novel potent and selective non-nucleotide antagonist of P2X$_3$ and P2X$_{2/3}$ receptors, reduces chronic inflammatory and neuropathic pain in the rat. *Proc. Natl. Acad. Sci. USA* **99**, 17179-17184.

Jiang, L. H., Kim, M., Spelta, V., Bo, X., Surprenant, A. and North, R. A. (2003). Subunit arrangement in P2X receptors. *J. Neurosci.* **23**, 8903-8910.

Jo, Y. H. and Schlichter, R. (1999). Synaptic corelease of ATP and GABA in cultured spinal neurons. *Nat. Neurosci.* **2**, 241-245.

Johansen, F. F., Lambolez, B., Audinat, E., Bochet, P. and Rossier, J. (1995). Single cell RT-PCR proceeds without the risk of genomic DNA amplification. *Neurochem. Int.* **26**, 239-243.

Kamphuis, W., Klooster, J. and Dijk, F. (2003). Expression of AMPA-type glutamate receptor subunit (GluR2) in ON-bipolar neurons in the rat retina. *J. Comp. Neurol.* **455**, 172-186.

Kanjhan, R., Housley, G. D., Thorne, P. R., Christie, D. L., Palmer, D. J., Luo, L. and Ryan, A. F. (1996). Localization of ATP-gated ion channels in cerebellum using P2x$_2$R subunit-specific antisera. *Neuroreport* **7**, 2665-2669.

Kanjhan, R., Raybould, N. P., Jagger, D. J., Greenwood, D. and Housley, G. D. (2003). Allosteric modulation of native cochlear P2X receptors: insights from comparison with recombinant P2X$_2$ receptors. *Audiol. Neurootol.* **8**, 115-128.

Khakh, B. S. and Egan, T. M. (2005). Contribution of transmembrane regions to ATP-gated P2X$_2$ channel permeability dynamics. *J. Biol. Chem.* **280**, 6118-6129.

Khakh, B. S. and North, R. A. (2006). P2X receptors as cell surface ATP sensors in health and disease. *Nature* **442**, 527-532.

Khakh, B. S., Burnstock, G., Kennedy, C., King, B. F., North, R. A., Seguela, P., Voigt, M. and Humphrey, P. P. (2001). International union of pharmacology. XXIV. Current status of the nomenclature and properties of P2X receptors and their subunits. *Pharmacol. Rev.* **53**, 107-118.

King, B. F., Ziganshina, L. E., Pintor, J. and Burnstock, G. (1996). Full sensitivity

of P2X$_2$ purinoceptor to ATP revealed by changing extracellular pH. *Br. J. Pharmacol.* **117**, 1371-1373.

Lewis, C., Neidhart, S., Holy, C., North, R. A., Buell, G. and Surprenant, A. (1995). Coexpression of P2X$_2$ and P2X$_3$ receptor subunits can account for ATP-gated currents in sensory neurons. *Nature* **377**, 432-435.

Liss, B., Franz, O., Sewing, S., Bruns, R., Neuhoff, H. and Roeper, J. (2001). Tuning pacemaker frequency of individual dopaminergic neurons by Kv4.3L and KChip3.1 transcription. *EMBO J.* **20**, 5715-5724.

Liu, M., King, B. F., Dunn, P. M., Rong, W., Townsend-Nicholson, A. and Burnstock, G. (2001). Coexpression of P2X$_3$ and P2X$_2$ receptor subunits in varying amounts generates heterogeneous populations of P2X receptors that evoke a spectrum of agonist responses comparable to that seen in sensory neurons. *J. Pharmacol. Exp. Ther.* **296**, 1043-1050.

McGuinness, S. L. and Shepherd, R. K. (2005). Exogenous BDNF rescues rat spiral ganglion neurons in vivo. *Otol. Neurotol.* **26**, 1064-1072.

Mou, K., Hunsberger, C. L., Cleary, J. M. and Davis, R. L. (1997). Synergistic effects of BDNF and NT-3 on postnatal spiral ganglion neurons. *J. Comp. Neurol.* **386**, 529-539.

Nicke, A., Baumert, H. G., Rettinger, J., Eichele, A., Lambrecht, G., Mutschler, E. and Schmalzing, G. (1998). P2X$_1$ and P2X$_3$ receptors form stable trimers: a novel structural motif of ligand-gated ion channels. *EMBO J.* **17**, 3016-3028.

Nikolic, P., Housley, G. D., Luo, L., Ryan, A. F. and Thorne, P. R. (2001). Transient expression of P2X$_1$ receptor subunits of ATP-gated ion channels in the developing rat cochlea. *Brain Res. Dev. Brain Res.* **126**, 173-182.

Nikolic, P., Housley, G. D. and Thorne, P. R. (2003). Expression of the P2X$_7$ receptor subunit of the adenosine 5'-triphosphate-gated ion channel in the developing and adult rat cochlea. *Audiol. Neurootol.* **8**, 28-37.

North, R. A. (2002). Molecular physiology of P2X receptors. *Physiol. Rev.* **82**, 1013-1067.

Pfaffl, M. W., Georgieva, T. M., Georgiev, I. P., Ontsouka, E., Hadeleit, M. and Blum, J. W. (2002). Real-time RT-PCR quantification of insulin-like growth factor (IGF)-1, IGF-1 receptor, IGF-2, IGF-2 receptor, insulin receptor, growth hormone receptor, IGF-binding proteins 1, 2 and 3 in the bovine species. *Domest. Anim. Endocrinol.* **22**, 91-102.

Pirvola, U. and Ylikoski, J. (2003). Neurotrophic factors during inner ear development. *Curr. Top. Dev. Biol.* **57**, 207-223.

Pujol, R., Lavigne-Rebillard, M. and Lenoir, M. (1998). Development of sensory and neural structures in the mammalian cochlea. In *Development of the Auditory System* (ed. E. W. Rubel, A. N. Popper and R. R. Fay), pp. 146-192. New York: Springer.

Rubel, E. W. and Fritzsch, B. (2002). Auditory system development: primary auditory neurons and their targets. *Annu. Rev. Neurosci.* **25**, 51-101.

Ryan, A. F., Wittig, J., Evans, A., Dazert, S. and Mullen, L. (2006). Environmental micro-patterning for the study of spiral ganglion neurite guidance. *Audiol. Neurootol.* **11**, 134-143.

Salih, S. G., Housley, G. D., Burton, L. D. and Greenwood, D. (1998). P2X$_2$ receptor subunit expression in a subpopulation of cochlear type I spiral ganglion neurones. *Neuroreport* **9**, 279-282.

Salih, S. G., Jagger, D. J. and Housley, G. D. (2002). ATP-gated currents in rat primary auditory neurones in situ arise from a heteromultimetric P2X receptor subunit assembly. *Neuropharmacology* **42**, 386-395.

Simmons, D. D., Manson-Gieseke, L., Hendrix, T. W., Morris, K. and Williams, S. J. (1991). Postnatal maturation of spiral ganglion neurons: a horseradish peroxidase study. *Hear. Res.* **55**, 81-91.

Stoop, R., Surprenant, A. and North, R. A. (1997). Different sensitivities to pH of ATP-induced currents at four cloned P2X receptors. *J. Neurophysiol.* **78**, 1837-1840.

Sucher, N. J., Deitcher, D. L., Baro, D. J., Warrick, R. M. and Guenther, E. (2000). Genes and channels: patch/voltage-clamp analysis and single-cell RT-PCR. *Cell Tissue Res.* **302**, 295-307.

Wagatsuma, A., Sadamoto, H., Kitahashi, T., Lukowiak, K., Urano, A. and Ito, E. (2005). Determination of the exact copy numbers of particular mRNAs in a single cell by quantitative real-time RT-PCR. *J. Exp. Biol.* **208**, 2389-2398.

Wangemann, P. (1996). Ca^{2+}-dependent release of ATP from the organ of Corti measured with a luciferin-luciferase bioluminescence assay. *Aud. Neurosci.* **2**, 187-192.

Warrington, J. A., Nair, A., Mahadevappa, M. and Tsyganskaya, M. (2000). Comparison of human adult and fetal expression and identification of 535 housekeeping/maintenance genes. *Physiol. Genomics* **2**, 143-147.

Wildman, S. S., Brown, S. G., Rahman, M., Noel, C. A., Churchill, L., Burnstock, G., Unwin, R. J. and King, B. F. (2002). Sensitization by extracellular Ca^{2+} of rat P2X$_5$ receptor and its pharmacological properties compared with rat P2X$_1$. *Mol. Pharmacol.* **62**, 957-966.

Xiang, Z., Bo, X. and Burnstock, G. (1999). P2X receptor immunoreactivity in the rat cochlea, vestibular ganglion and cochlear nucleus. *Hear. Res.* **128**, 190-196.

Zhan, G., Shaheen, F., Mackiewicz, M., Fenik, P. and Veasey, S. C. (2002). Single cell laser dissection with molecular beacon polymerase chain reaction identifies 2A as the predominant serotonin receptor subtype in hypoglossal motoneurons. *Neuroscience* **113**, 145-154.